

# Similarities and differences of copper and zinc cations binding to biologically relevant peptides studied by vibrational spectroscopies

Alicia Schirer<sup>1</sup> · Youssef El Khoury<sup>1</sup> · Peter Faller<sup>2</sup> · Petra Hellwig<sup>1</sup>

Received: 1 December 2016 / Accepted: 3 March 2017 / Published online: 20 March 2017  
© SBIC 2017

**Abstract** GHK and DAHK are biological peptides that bind both copper and zinc cations. Here we used infrared and Raman spectroscopies to study the coordination modes of both copper and zinc ions, at pH 6.8 and 8.9, correlating the data with the crystal structures that are only available for the copper-bound form. We found that Cu(II) binds to deprotonated backbone (amidate), the N-terminus and N<sup>π</sup> of the histidine side chain, in both GHK and DAHK, at pH 6.8 and 8.9. The data for the coordination of zinc at pH 6.8 points to two conformers including both nitrogens of a histidine residue. At pH 8.9, vibrational spectra of the ZnGHK complexes show that equilibria between monomers, oligomers exist, where deprotonated histidine residues as well as deprotonated amide nitrogen are involved in the coordination. A common feature is found: zinc cations coordinate to N<sup>π</sup> and/or N<sup>π</sup> of the His leading to the formation of GHK and DAHK multimers. In contrast, Cu(II) binds His via N<sup>π</sup> regardless of the peptide, in a pH-independent manner.

**Keywords** Infrared spectroscopy · Raman spectroscopy · GHK · DAHK · Peptide copper coordination · Zinc coordination

## Abbreviations

FTIR	Fourier transform infrared
GHK	NH <sub>2</sub> -Glycine-histidine-lysine-COOH
DAHK	NH <sub>2</sub> -Aspartic acid-alanine-histidine-lysine-COOH
HSA	Human serum albumin
$\nu$	Stretching vibration
$\delta$	In-plane bending vibration
$\omega$	Wagging vibration

## Introduction

Copper and zinc cations are two ubiquitous d-block metals in living cells. The human serum albumin protein (HSA) binds and transports Zn(II) and Cu(II) ions in the blood. HSA has distinct high-affinity binding sites for the two cations [1]. Cu(II) is bound to the N-terminus [2, 3] and the binding site is formed by the first three amino acids (i.e., Asp, His, and Gly): one His, two amidates (deprotonated amide nitrogen) and the N-terminal amine function form the first coordination sphere. This binding site can be mimicked by the tetra-peptide DAHK which binds Cu with the same ligands and for which the crystal structure is known [4]. The zinc high-affinity binding site (Site A) is at the interface between the so-called domains I and II of HSA [5, 6]. Zn(II) is bound in a tetrahedral geometry to two His, one Asp, and a water molecule at pH 9.0. The N-terminus of HSA is known for binding Cu(II) and Ni(II) cations, nevertheless Zn(II) can be weakly bound at pH higher than the physiological one [7]. Beside HSA, a tripeptide formed by Gly, His and Lys (GHK) is found in the plasma. It is a high-affinity chelator of Cu(II) and it mediates the transport of Cu(II) to the cells, hence promoting their growth [8]. Moreover, CuGHK complex seems to improve the skin

A. Schirer and Y. El Khoury contributed equally to this work.

✉ Petra Hellwig  
hellwig@unistra.fr

<sup>1</sup> Laboratoire de bioélectrochimie et spectroscopie, UMR 7140, université de Strasbourg, 4 Rue Blaise Pascal, 67000 Strasbourg, France

<sup>2</sup> Laboratoire de biométaux et chimie biologique, UMR 7177, université de Strasbourg, 4 Rue Blaise Pascal, 67000 Strasbourg, France

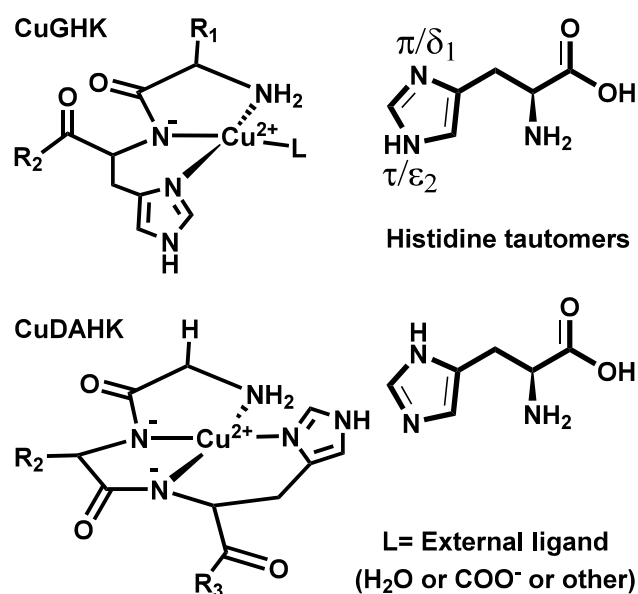


**Fig. 1** Structures of the CuGHK and CuDAHk complexes determined at pH 7.4 (*left*) [4]. The two Histidine tautomers (*right*) and the most commonly nomenclatures of the nitrogen atoms of the imidazole ring. Throughout the text, the  $\text{N}^\pi$  and  $\text{N}^\tau$  are used according to the IUPAC recommendation [17]

regeneration [9], participates in reversing gene expression in emphysema [10], plays a critical role against cognitive decline [11] and to be an adjuvant in cancer treatment [12].

GHK and DAHK are the canonical peptides of the motifs Xxx-His and Xxx-Xxx-His, and this motifs occur in a lot of peptides and proteins. Due to their crucial roles, copper-GHK (CuGHK) and copper-DAHk (CuDAHk) complexes have attracted major attention and were studied by several techniques [13–15]. The structures of both complexes have been resolved by X-ray crystallography (Fig. 1) [4, 16]. Less is known about the binding of Zn(II) to these peptides. It is therefore important to shed more light on the coordination of Zn(II) in comparison to Cu(II), both, near physiological pH as well as at basic pH since Zn(II) might bind differently at basic pH.

Copper and zinc ions are vital for living cells; the disruption of their homeostases is connected to neurodegenerative diseases such as Alzheimer, where copper and zinc ions are known to promote the aggregation of the amyloid beta peptides [18–20]. The neurotoxicity of these metals can be decreased by chelators [21] and the soluble peptides GHK and DAHK could be potent in protecting the neurons from Alzheimer's since they are better chelators of Cu(II) than amyloid beta peptides [22–25].

Here we studied these peptides by means of IR and Raman spectroscopies. First the vibrational signature of the Cu(II) complexes was correlated with the known X-ray structures. Then the coordination modes of Zn(II) cations

in both GHK and DAHK were identified. The binding modes of the His imidazole residues ( $\text{N}^\tau$  or  $\text{N}^\pi$ ) as well as their protonation state were obtained and it was possible to link the coordination modes to the biological relevance of the complexes in a pH-dependent manner [26–29].

## Materials and methods

### Sample preparation

GHK peptide was purchased from Bachem (Switzerland) and DAHK peptide was purchased from Bachem (Switzerland) or Genecust (Dudelange, Luxembourg). TFA (trifluoroacetic acid) was removed by lyophilization and HCl treatment [30]. The stock solutions were prepared by dissolving the peptides in distilled water. The pH was adjusted by adding of small amounts of HCl or NaOH.

The concentration of DAHK and GHK was determined by titration of Cu(II) using a UV/visible Cary 300 Spectrometer. First a stock solution was diluted 50-fold and amounts of Cu(II) solution of known concentration were added until no further increase in the d–d band of the Cu–peptide complex was observed. For CuGHK, the d–d band is at 607 nm and for CuDAHk, it is at 520 nm.

In order to add the cations,  $\text{ZnCl}_2$  (Sigma-Aldrich) and  $\text{CuCl}_2 \cdot \text{H}_2\text{O}$  (Riedel-de-Haen), respectively, were dissolved in distilled water to obtain a final concentration of 10 mM. They were stored at 4 °C.

### Raman spectroscopy

Raman spectra were recorded on a Renishaw in via Raman microscope equipped with a CCD (charge coupled device) detector. Samples were excited with the 514 nm line of an argon laser where the output power was set to 16.5 mW. A 50× objective was used to focus the laser onto the sample. Small droplets of 3  $\mu\text{L}$  were deposited on a  $\text{CaF}_2$  window and dried with a stream of argon. Several accumulations were averaged with an exposure time of 10 s, for each sample.

### Infrared (IR) spectroscopy

IR spectra were recorded on a Vertex 70 spectrometer (Bruker Optics, Germany) equipped with a Harrick-Diamond ATR, a Globar™ source and an MCT detector. For each sample, 10 spectra with 256 scans each were averaged. The spectral resolution was 4  $\text{cm}^{-1}$ .

The dried films used in these studies do not allow the normalization of the vibrational spectra.

## Results and discussion

The data shown below concerns dried films of GHK, DAHK and their corresponding Cu(II) and Zn(II) complexes at pH 6.8 and 8.9. The samples have been dried for several reasons, including the strong infrared absorption band of water that overlaps with the peptide signals in the amide I range. For Raman spectroscopy, dried films were used because of the absence of scattering signal of the studied samples in solution under the experimental conditions. Importantly, concentrated peptides can occur in vivo, for instance in amyloids, like the amyloid plaques found in Alzheimer's disease, which have also high concentrations of Zn bound to His. In addition X-ray structures are typically made from highly concentrated samples.

### FTIR data on GHK at pH 6.8 and 8.9

The infrared spectrum of GHK at pH 6.8 shows the amide I band centered at  $1657\text{ cm}^{-1}$  (Fig. 2). The amide I signal includes the  $\nu$  (C=O) vibration of the peptide backbone [31]. At pH 6.8, the coordination of Zn(II) slightly downshifts the maximum towards  $1652\text{ cm}^{-1}$ , whereas the

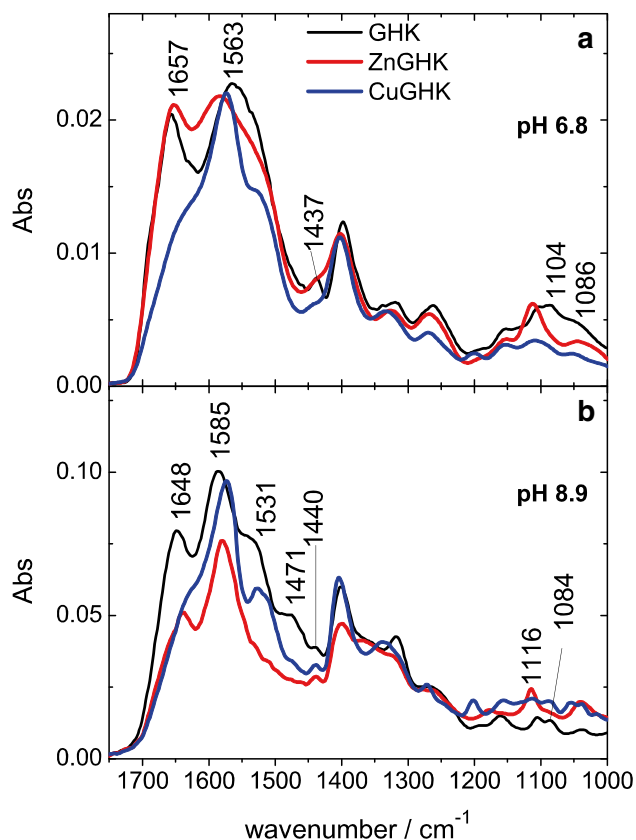


**Fig. 2** FTIR absorption spectra of free GHK (black trace) and its copper (blue trace) and zinc (red trace) complexes at pH 6.8 (a) and 8.9 (b) in the  $1750\text{--}1000\text{ cm}^{-1}$  spectral range

coordination of Cu(II) leads to a loss of the amide I modes to a large extent (Fig. 2a). This behavior means that the tripeptide undergoes a drastic change caused by the loss of the amide-like structure of the backbone via the binding of either the oxygen of the C=O or the nitrogen of the C–N of the backbone. According to the structure obtained in solution [4], one amidate is bound to Cu(II), whereas the binding of Zn(II) does not involve an amidate. This is in line with the amide I signature observed here. Note that the backbone nitrogen can bind Cu(II) or Zn(II) only if it is deprotonated (amidate).

In addition to the amide II vibrational modes that involves the coupled CN and NH vibrational modes from the backbone, [31] the  $1600\text{--}1520\text{ cm}^{-1}$  spectral range is dominated by the  $\nu$  (COO<sup>−</sup>)<sup>as</sup> vibration of the carboxylate of Lys as well as the  $\nu$  (C<sub>4</sub>=C<sub>5</sub>) vibration of His. The broad band centered at  $1563\text{ cm}^{-1}$  thus contains these different overlapping contributions. The complexation of Cu(II) by GHK induces a loss of the lower frequency fraction of this broad band which can be assigned to the amide II mode and only a shoulder remains at  $1526\text{ cm}^{-1}$ . This shoulder can be assigned to the  $\delta$  (NH<sub>3</sub><sup>+</sup>)<sup>s</sup> vibration of the Lys side chain [32]. A remaining narrow band is centered at  $1573\text{ cm}^{-1}$  and it can be assigned to the His  $\nu$  (C<sub>4</sub>=C<sub>5</sub>) or the Lys  $\nu$  (COO<sup>−</sup>)<sup>as</sup> vibrations. In the presence of Zn(II) cations the same band shifts to  $1584\text{ cm}^{-1}$ .

In order to study the interaction of the His residues by means of FTIR spectroscopy, it is important to study the spectral region around  $1100\text{ cm}^{-1}$  where the  $\nu$  (C5–N<sup>τ</sup>) vibration absorbs. This vibrational mode shows a high-sensitivity to metal binding as well as to the protonation state of His [33, 34]. The free peptide shows two bands at  $1104$  and  $1086\text{ cm}^{-1}$ , which can be assigned to the N<sup>π</sup> and N<sup>τ</sup> protonated forms, respectively. Upon Zn(II) binding a band is observed at  $1114\text{ cm}^{-1}$ . This band is a marker of metal binding via N<sup>τ</sup> while N<sup>π</sup> is protonated [33]. Accordingly, in the free form, the two tautomers of His are in equilibrium and Zn(II) coordination takes place via N<sup>τ</sup>. The Cu(II) complex shows a band at  $1108\text{ cm}^{-1}$ , difficult to discriminate from the one observed for the free form at  $1104\text{ cm}^{-1}$ ; thus, so far no accurate assignment can be made.

Raising the pH to 8.9 leads to a strong decrease the intensity of the amide I band upon metal binding (Fig. 2b) which is most likely due to the deprotonation of the amide function and the binding of the metal cations by the amidate. The ZnGHK complex shows a remaining well-defined band at  $1639\text{ cm}^{-1}$  which might be explained by the formation of a 1:2 complex (Zn:GHK) where one of the two peptide remains in the protonated amide form. Another explanation is the presence of an equilibrium between 1:1 complexes where a mixture of protonated and deprotonated charged amide functional groups coexist. In contrast to pH 6.8, the amide II band is narrow at pH

8.9 and downshifts from 1586 to 1573  $\text{cm}^{-1}$  upon Cu(II) binding and to 1579  $\text{cm}^{-1}$  upon Zn(II) binding. The signal at 1531  $\text{cm}^{-1}$  can be assigned to the  $\delta(\text{NH}_3^+)^s$  vibration of the Lys side chain. The basic pH value is very close the  $\text{pK}_a$  of the  $\text{NH}_3^+/\text{NH}_2$  which means that the two forms coexist. This signal disappears only upon Zn(II) binding, suggesting that the equilibrium is shifted towards a neutral amine. Moreover, it is not excluded that the amine of the Lys residue contributes to the binding of Zn(II) ions. The spectral region from 1400 to 1200  $\text{cm}^{-1}$  contains the  $\delta(\text{CH}_2)$ ,  $\omega(\text{CH}_2)$  as well as the His ring  $\nu(\text{C}-\text{N})$  vibrations [32].

The two tautomeric forms of the free His side chain can be detected at pH 8.9 via the  $\nu(\text{C}5-\text{N}^\tau)$  vibrations at 1105 and 1084  $\text{cm}^{-1}$ . They are replaced by a single band at 1115  $\text{cm}^{-1}$  upon Zn(II) binding, corresponding to the  $\text{N}^\tau$  binding while  $\text{N}^\pi$  is protonated. In order to confirm and complete these findings, Raman spectra of the same samples have been studied in comparable experimental conditions (see “Materials and methods”).

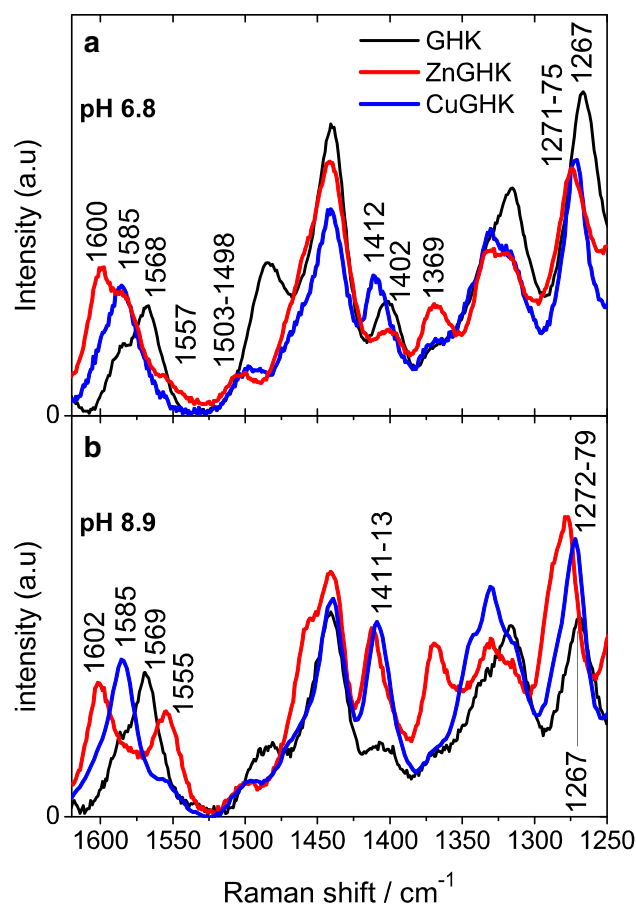
### Raman data on GHK at pH 6.8 and 8.9

Figure 3a shows the Raman spectra of free and metal-bound GHK at pH 6.8. In the spectrum of free peptide, two bands tentatively assigned to the His  $\nu(\text{C}_4=\text{C}_5)$  vibration can be observed at 1585 and 1568  $\text{cm}^{-1}$ . These bands correspond to the  $\text{N}^\pi$  and  $\text{N}^\tau$  protonated form, respectively [33]. Thus, it suggests that the His residue adopts either protonation state in free GHK at pH 6.8.

When Cu(II) binds to the tripeptide, the signal at 1568  $\text{cm}^{-1}$  disappears and the band appearing at 1585  $\text{cm}^{-1}$  gains intensity showing that all the His residues in the sample adopt the  $\text{N}^\tau$  protonation state while binding Cu(II) with  $\text{N}^\pi$ . Importantly, upon Zn(II) binding, two bands appear at 1600 and 1585  $\text{cm}^{-1}$ . The former one is assigned to the  $\nu(\text{C}_4=\text{C}_5)$  vibration of the  $\text{N}^\tau$ -bound form. The latter one can be assigned to the  $\nu(\text{C}_4=\text{C}_5)$  vibration of the  $\text{N}^\pi$ -bound form.

Cu(II) and Zn(II) chelation causes the appearance of a shoulder at 1557  $\text{cm}^{-1}$ , overlapped by the band at 1569  $\text{cm}^{-1}$  in the Raman spectrum of the free peptide. This band is assigned to  $\nu(\text{COO}^-)^{\text{as}}$  vibrations of Lys. The corresponding  $\nu(\text{COO}^-)^s$  vibration occurs around 1400  $\text{cm}^{-1}$ . The shoulder observed at around 1360  $\text{cm}^{-1}$  in Fig. 3a for the free and CuGHK complexes becomes sharper upon Zn binding. The accurate assignment of this band is not possible due to potential overlaps. For instance it can be arising from the  $\nu(\text{COO}^-)^s$  vibration of Lys, however, isotope labeling and simulation can help providing a more accurate assignment.

A second marker for His can be seen for the free peptide in Fig. 3b at 1267  $\text{cm}^{-1}$  (His ring breathing mode).



**Fig. 3** Raman spectra of free GHK (black trace) and its copper (blue trace) and zinc (red trace) complexes at pH 6.8 (a) and 8.9 (b) in the 1620–1250  $\text{cm}^{-1}$  spectral ranges

This band upshifts to 1271 and 1275  $\text{cm}^{-1}$  upon Cu(II) and Zn(II) binding, respectively. This band is a marker of  $\text{N}^\tau$  coordination while  $\text{N}^\tau$  is protonated [27, 28].

The Cu(II) binding to amidate observed by FTIR spectroscopy is in line with the modification observed in the region 1486–1410  $\text{cm}^{-1}$  where the  $\text{CO}/\text{CN}^-$  vibrations are observed, including the upshift and increase of the band at 1402  $\text{cm}^{-1}$ .

So far, markers for both binding forms of the His are observed for ZnGHK in Fig. 3a which suggests either the formation of 1:2 Zn:GHK complex or an equilibrium between the two forms (most likely hypothesis). For CuGHK, we can conclude that the coordination takes place via  $\text{N}^\tau$  which is in line with the previously published structure [4].

The spectrum of free GHK at pH 8.9 is very similar to the one at pH 6.8 (Fig. 3b). The Cu(II) binding seems to take place via  $\text{N}^\tau$  since the  $\nu(\text{C}_4=\text{C}_5)$  vibration of His occurs at 1585  $\text{cm}^{-1}$ . The ZnGHK complex exhibits a band at 1602  $\text{cm}^{-1}$  which is typical of  $\text{N}^\tau$  metal binding His. This broad band may also involve the small contribution

from the  $N^{\pi}$ -bound His, nevertheless, the  $N^{\tau}$ -bound form remains the major component. In addition, the intensity of the signal at  $1555\text{ cm}^{-1}$  increases upon binding, reflecting the presence of the metal bridging imidazolate [28, 35, 36].

In the literature, the band at  $1555\text{ cm}^{-1}$  is associated with the one found around  $1290\text{ cm}^{-1}$ , which in this case is probably overlapping with the band at  $1278\text{ cm}^{-1}$ . The signal of the bridging imidazolate at  $1555\text{ cm}^{-1}$  increased considerably at pH 11 (not shown) and this observation supports the formation of a ZnGHK oligomeric complex with one His binding via  $N^{\pi}$  and  $N^{\tau}$ . Accordingly, the equilibrium between the two 1:1 conformers is shifted towards forming an oligomeric complex at high pH. It is noted that a deprotonated His residue is not commonly observed for metal–His complexes in solution. It is more likely to find a deprotonated His in dry films, as it is the case here.

A strong band can be observed at  $1411$  or  $1413\text{ cm}^{-1}$  upon Cu(II) and Zn(II) binding, respectively, suggesting the involvement of amide nitrogen in metal binding. The observation of the coordination of a bridging His and the amidate in the same Zn(II) complex is rather surprising. It is noted, however, that this binding mode was reported before [37, 38]. The His marker band at  $1267\text{ cm}^{-1}$  (His ring breathing mode [27]) upshifts and gains intensity in both complexes which is an indication of metal binding via  $N^{\pi}$ . Accordingly, the ZnGHK sample at pH 8.9 exhibits an equilibrium between 1:1 and 2:2 Zn:GHK complexes involving either N atoms of the His residue in the monomer and both N atoms from imidazolate, the amidate from the backbone as well as either N atoms from a neutral His in 2:2 Zn:peptide complexes. The comparison between the observed coordination modes in CuGHK, ZnGHK and the available structure of CuGHK is summarized in Table 1.

### FTIR data on DAHK at pH 6.8 and 8.9

The FTIR spectra of DAHK (Fig. 4) are highly similar to the ones of GHK and metal binding has similar effects on the spectral signature. For instance Cu(II) binding at pH 6.8 induces the loss of the signal at  $1654\text{ cm}^{-1}$ , whereas

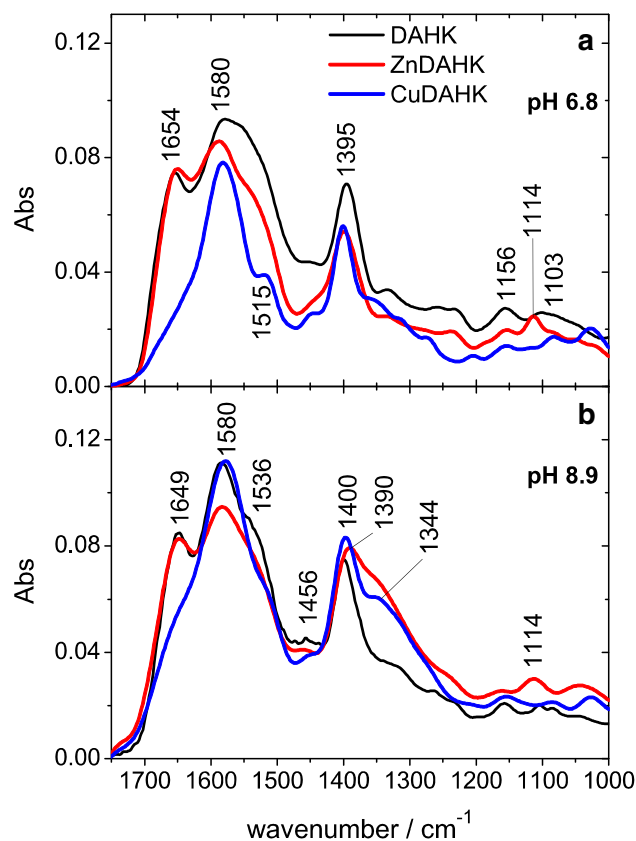


**Fig. 4** FTIR absorption spectra of free DAHK (black trace) and its copper (blue trace) and zinc (red trace) complexes at pH 6.8 (a) and 8.9 (b) in the  $1750\text{--}1000\text{ cm}^{-1}$  spectral range

**Table 1** Binding partners and marker bands of copper and zinc in GHK as a function of pH as detected with vibrational spectroscopy and compared to the X-ray and solution structures [4]

	CuGHK			ZnGHK					
	pH 6.8	pH 8.9	X-ray	pH 7.4	Solution	Vibrational marker	pH 6.8	pH 8.9	Vibrational marker
$N^{\pi}$	✓	✓	✓			$\nu$ ( $C_4=C_5$ ), ring breathing (Raman)	✓	✓	$\nu$ ( $C_4=C_5$ ), ring breathing (Raman)
$N^{\tau}$							✓	✓	$\nu$ ( $C_4=C_5$ ), Ring breathing (Raman)
Gly ( $NH_2$ )			✓		✓				
Gly-His (amidate)	✓	✓	✓		✓	Amide I loss (IR)		✓	Amide I loss (IR)
Lys ( $COO^-$ )			✓						
Exogenous ( $COO^-/H_2O$ )					✓				

Note that in the solid state the CuGHK complex is a dimer, but a monomer in solution in which the fourth ligand is suggested to be provided by exogenous acetate or a water molecule

no significant changes occur upon Zn(II) binding which is an indicator of the amidate binding to Cu(II) but not to Zn(II). His binding to Zn(II) is analogous to GHK (via  $N^{\tau}$  while  $N^{\pi}$  is protonated) as suggested by the signal at  $1114\text{ cm}^{-1}$  (Fig. 4a). Upon Cu(II) binding, the broad signal at  $1546\text{ cm}^{-1}$  loses intensity and a weaker signal remains at  $1515\text{ cm}^{-1}$ . This signal can be assigned to the  $\delta$  ( $\text{NH}_3^+$ ) $^s$  vibration of Lys that does not bind Cu(II) while the lost signal probably originates from the amidate binding.

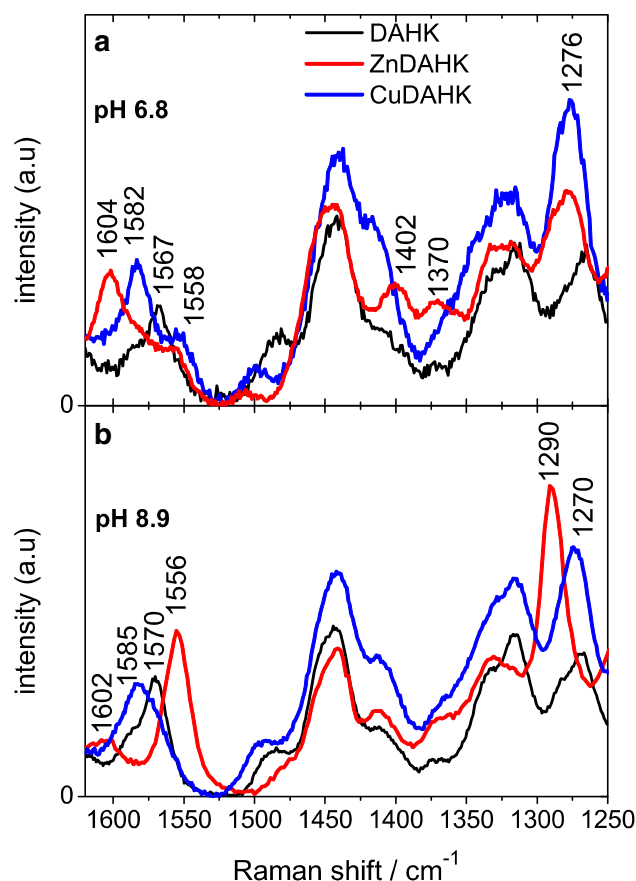
At pH 8.9 (Fig. 4b) a new band appears at  $1344\text{ cm}^{-1}$  in the spectra of the complexes. This band can be assigned to the  $\nu$  ( $\text{COO}^-$ ) $^s$  vibration of the Asp side chain. Yet, the corresponding  $\nu$  ( $\text{COO}^-$ ) $^{\text{as}}$  vibration that usually occurs around  $1580\text{ cm}^{-1}$  cannot be clearly identified in the corresponding spectra due to spectral crowding. Moreover, the  $\nu$  ( $\text{COO}^-$ ) $^s$  vibration occurs usually around  $1400\text{ cm}^{-1}$ , i.e., on a significantly higher frequencies than the observed ones, and an unambiguous assignment can only be made with the help of  $^{13}\text{C}$  isotope labeling of Asp1.

### Raman spectra of DAHK at pH 6.8 and 8.9

The Raman spectrum of free DAHK recorded at pH 6.8 shows a signal at  $1567\text{ cm}^{-1}$  (Fig. 5a). The binding of Cu(II) induces an upshift of this band to  $1582\text{ cm}^{-1}$  that can be assigned it to the  $\nu$  ( $\text{C}_4=\text{C}_5$ ) vibration of the  $N^{\pi}$  His-bound form. The shoulder seen at  $1558\text{ cm}^{-1}$  is most likely arising from the  $\nu$  ( $\text{COO}^-$ ) $^{\text{as}}$  vibration of Lys and Asp. Zn(II) chelation at pH 6.8 is accompanied by the appearance of the  $\nu$  ( $\text{C}_4=\text{C}_5$ ) vibration of the  $N^{\tau}$  His-bound form at  $1604\text{ cm}^{-1}$  as well as a signal at  $1558\text{ cm}^{-1}$ . The signals at  $1402$  and  $1370\text{ cm}^{-1}$  in the spectrum of ZnDAHK are present in the spectrum of the free peptide but gain intensity upon Zn binding. The assignment of these signals is not straightforward (same as for ZnGHK at pH 6.8); isotopic labeling and simulations can help with the assignment.

Moreover, the band at  $1269\text{ cm}^{-1}$  from free DAHK upshifts to  $1276\text{ cm}^{-1}$  upon metal binding. Its increase in intensity points towards the binding to His via  $N^{\tau}$ , an observation that is in line with the crystal structure of CuDAHK [4].

The Raman spectra obtained after Cu(II) binding at pH 8.9 (Fig. 5b) are very similar to those seen at pH 6.8. The bands at  $1585$  and  $1270\text{ cm}^{-1}$  confirm the binding to His via  $N^{\tau}$ . In contrast, Zn(II) binding shows a weak band at  $1602\text{ cm}^{-1}$  which is a marker of the His coordination via  $N^{\tau}$  [27, 34]. The intensity of this band reflects the binding of a small fraction of His residues to Zn(II) via  $N^{\tau}$ . At pH 8.9, the spectrum of the ZnDAHK complex exhibits two intense bands at  $1556$  and  $1290\text{ cm}^{-1}$  which represent the signature of the deprotonated

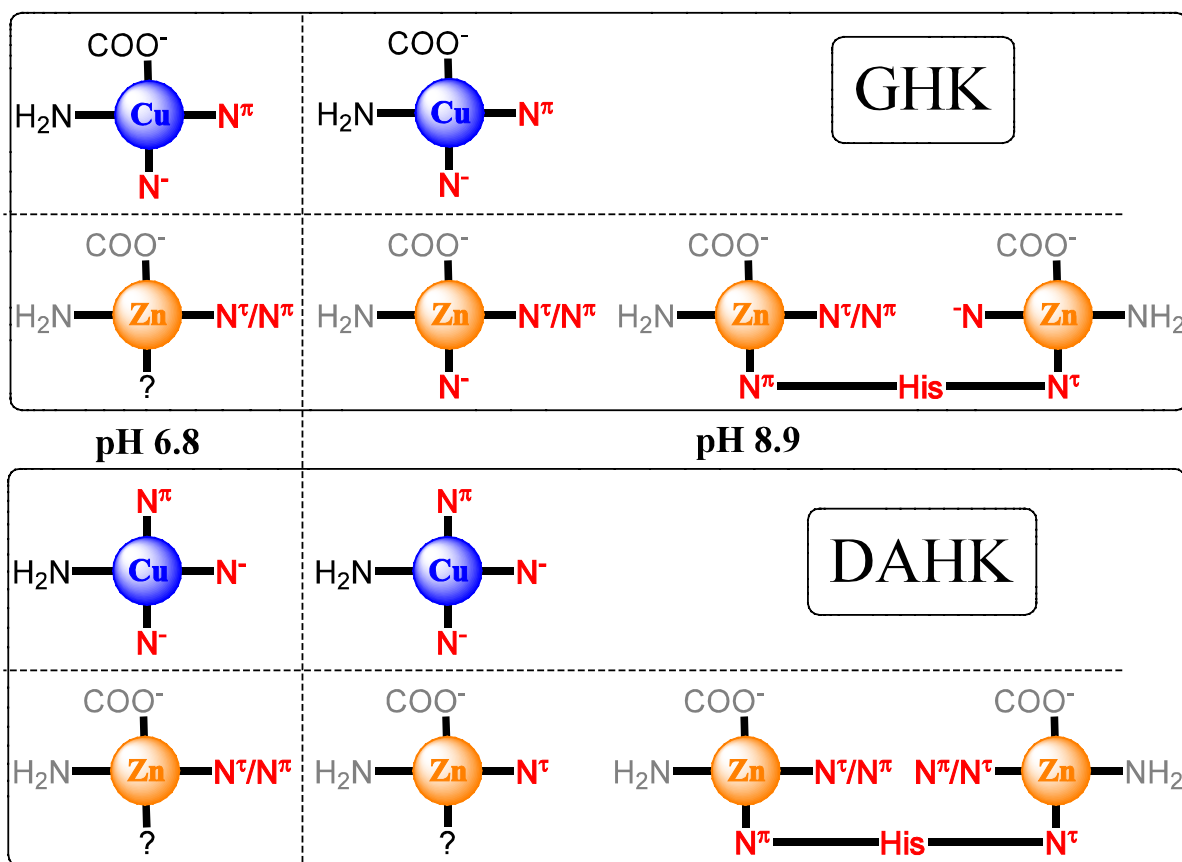


**Fig. 5** Raman spectra of free DAHK (black trace) and its copper (blue trace) and zinc (red trace) complexes at pH 6.8 (a) and 8.9 (b) in the  $1620\text{--}1250\text{ cm}^{-1}$  spectral ranges

imidazole of His bound to metal cations via both,  $N^{\tau}$  and  $N^{\pi}$  [28]. The high-frequency mode is assigned to the  $\nu$  ( $\text{C}_4=\text{C}_5$ ) vibration, whereas the low-frequency signal is assigned to the ring breathing mode. Table 2 shows a comparison between the observed coordination modes in CuDAHK, ZnDAHK and the available structure. Altogether, the spectra at pH 8.9 point towards equilibrium of two complexes. In one, the binding occurs via  $N^{\tau}$  while  $N^{\pi}$  is protonated and in the other a fully deprotonated His coordinates via the two nitrogen atoms. Based on the low intensity of the marker band of the neutral form of His, it is very likely that the equilibrium is shifted towards the fully deprotonated imidazole. This is confirmed by measurements done at pH 11 where only the fully deprotonated form is observed (data not shown). We can suggest that an oligomeric complex is formed at pH 8.9 where one His binds via  $N^{\pi}$  and  $N^{\tau}$  while the other His binds via either N atom. This is an intriguing observation since two Zn(II) cations would be very close to each other.

**Table 2** Binding partners and marker bands of copper and zinc in DAHK as a function of pH as detected with vibrational spectroscopy and compared to the X-ray and solution structures [4]

	CuDAHK				Vibrational marker	ZnDAHK		
	pH 6.8	pH 8.9	X-ray pH 7.4	Solution		pH 6.8	pH 8.9	Vibrational marker
N <sup>π</sup>	✓	✓	✓		$\nu$ (C <sub>4</sub> =C <sub>5</sub> ) (Raman)	✓	✓	$\nu$ (C <sub>4</sub> =C <sub>5</sub> ) (Raman)
N <sup>τ</sup>						✓	✓	$\nu$ (C <sub>4</sub> =C <sub>5</sub> ) (Raman)
Asp (NH <sub>2</sub> )			✓	✓				
Backbone (amidate)	✓	✓	✓	✓	Amide I loss (IR)			
Asp (COO <sup>-</sup> )								
H <sub>2</sub> O			✓	✓				

**Fig. 6** Suggested coordination spheres for Zn(II) and Cu(II) GHK and DAHK complexes as a function of pH in a dried film as deduced from FTIR and Raman spectroscopies. Binding partners detected with vibrational spectroscopies are noted in *red* (for Zn(II) and Cu(II) complexes), those suggested from X-ray structure of CuGHK and CuDAHK complexes are marked in *black* and other proposed ligand

for Zn in analogy to the X-ray and solution structures of the Cu(II) complexes are marked in *grey*. Note that the cartoon indicates the involved ligands. It does not mean that all shown ligands are bound simultaneously due to the presence of different species. For the oligomers, the coordination of only two Zn(II) cations of an oligomer are presented for clarity

## Conclusion

The FTIR and Raman spectra of two biologically important peptides, GHK and DAHK, bound to Cu(II) and Zn(II) divalent cations are reported in dried films at pH 6.8 and

8.9. In direct comparison to the available structures of the Cu(II) complexes at pH 7.4, we propose coordination spheres for the corresponding Zn(II) cations complexes. The difference between Zn(II) and Cu(II) binding to GHK at low pH is in the absence of coordination via the Gly-His

amidate for Zn(II). Furthermore, we report the presence of different complexes in equilibrium, since two coordination spheres involving His via  $N^\pi$  or  $N^\tau$  can be identified. At high pH, amidate becomes involved in the Zn(II) coordination and the  $N^\tau$ -bound form becomes the dominant complex. As the simultaneous binding of amidate and  $N^\tau$  is sterically not favorable (as compared to amidate and  $N^\pi$ ), it is likely that they do not bind to the same Zn(II). Moreover, the typical signature of deprotonated His appears in the Raman spectrum where a bridging oligomeric ZnGHK complex is formed and this signature becomes the dominant feature at pH 11 (not shown), which clearly indicates that the spectrum recorded at pH 8.9 mirrors the existence of an equilibrium between different forms.

The study of DAHK complexes by means of vibrational spectroscopies shows that Cu(II) binds His via  $N^\pi$  at low pH which is in line with the X-ray structure. At high pH, the coordination mode of the His remains the same, in line with spectroscopic data from the literature. No amidate binding was observed in the case of Zn(II) cations at pH 6.8 and the presence of an equilibrium between two 1:1 Zn:DAHK complexes involving His binding via  $N^\pi$  or  $N^\tau$  can be proposed. However, the  $N^\tau$ -bound form seems to be the main component. At pH 8.9, His partially deprotonates and zinc binding takes place via  $N^\pi$  and  $N^\tau$ , pointing towards an equilibrium between different forms while the formation of an oligomeric ZnDAHK complex remains major. The equilibrium is completely shifted towards the oligomeric form at pH 11.

The suggested coordination sphere transitions as a function of pH are shown in Fig. 6. As a common feature, regardless of the peptide, zinc cations always seem to coordinate to  $N^\tau$  and/or  $N^\pi$  of the His at the given experimental conditions. Accordingly GHK and DAHK tend to form zinc-peptide oligomeric complexes involving deprotonated His residues. In contrast, Cu(II) binds His via  $N^\pi$  regardless of the peptide and in a pH-independent manner. Such differences in behavior between the two metals originate from the different electronic configuration, Cu(II) is  $d^9$  and Zn(II) is  $d^{10}$ . Thus the two ions differ in their Lewis acidity and in their favored geometries of the respective complexes. Due to the Jahn–Teller effect of the  $d^9$  in Cu(II), this ion prefers a square planar coordination with one or two weaker axial ligands. Moreover, Cu(II) is a stronger Lewis acid (smaller ion radius and Jahn–Teller distortion) and hence is able to bind to amidates at neutral pH. Zn(II) is  $d^{10}$ , so there is no ligand-field stabilization energy and hence Zn(II) can adopt different geometries, but favors largely tetrahedral when tetra-coordinated.

The coordination CuDAHK with a square planar coordination environment including two amidates, is well adapted to Cu(II), but not for Zn(II). This favored Cu(II)

coordination is only possible when Cu is bound to the  $N^\tau$  of the His, because an entropically favored five-membered chelate ring is present (Fig. 1). It is noted that with  $N^\tau$  a less favored six-membered chelate ring would be formed. Similar reasoning applies also to GHK, but less pronounced as only one amidate binds. Zn(II), not able to bind amidate at neutral pH binds hence differently. Both  $N^\pi$  and  $N^\tau$  atoms of His are accessible for binding Zn ions (being more exposed,  $N^\tau$  may be a little favored over  $N^\pi$ ).

**Acknowledgements** A. Schirer, Y. El Khoury and P. Hellwig acknowledge the support by the University of Strasbourg, the CNRS as well as the FRC. P. Faller gratefully acknowledges the support of the University of Strasbourg and the University of Strasbourg Institute for Advanced Study (USIAS).

## References

- Bal W, Sokolowska M, Kurowska E, Faller P (2013) *Biochim Biophys Acta* 1830:5444–5455
- Masuoka J, Saltman P (1994) *J Biol Chem* 269:25557–25561
- Bal W, Christodoulou J, Sadler PJ, Tucker A (1998) *J Inorg Biochem* 70:33–39
- Hureau C, Eury H, Guillot R, Bijani C, Sayen S, Solari PL, Guillon E, Faller P, Dorlet P (2011) *Chemistry* 17:10151–10160
- Handing KB, Shabalin IG, Kassar O, Khazaipoul S, Blindauer CA, Stewart AJ, Chruszcz M, Minor W (2016) *Chem Sci* 7:6635–6648
- Stewart AJ, Blindauer CA, Berezenko S, Sleep D, Sadler PJ (2003) *Proc Natl Acad Sci U S A* 100:3701–3706
- Lakusta H, Sarkar B (1979) *J Inorg Biochem* 11:303–315
- Pickart L, Freedman JH, Loker WJ, Peisach J, Perkins CM, Stenkamp RE, Weinstein B (1980) *Nature* 288:715–717
- Pickart L, Vasquez-Soltero JM, Margolina A (2015) *Biomed Res Int*. doi:10.1155/2015/648108
- Campbell JD, McDonough JE, Zeskind JE, Hackett TL, Pechkovsky DV, Brandsma C-A, Suzuki M, Gosselink JV, Liu G, Alekseyev YO, Xiao J, Zhang X, Hayashi S, Cooper JD, Timens W, Postma DS, Knight DA, Lenburg ME, Hogg JC, Spira A (2012) *Genome Med* 4:67
- Pickart L, Vasquez-Soltero JM, Margolina A (2012) *Oxid Med Cell Longev* 2012:324832
- Hong Y, Downey T, Eu KW, Koh PK, Cheah PY (2010) *Clin Exp Metastasis* 27:83–90
- Trapaidze A, Hureau C, Bal W, Winterhalter M, Faller P (2012) *J Biol Inorg Chem* 17:37–47
- Conato C, Gavioli R, Guerrini R, Kozłowski H, Mlynarz P, Pasti C, Pulidori F, Remelli M (2001) *Biochim Biophys Acta* 1526:199–210
- Freedman JH, Pickart L, Weinstein B, Mims WB, Peisach J (1982) *Biochemistry* 21:4540–4544
- Perkins CM, Rose NJ, Weinstein B, Stenkamp RE, Jensen LH, Pickart L (1984) *Inorg Chim Acta* 82:93–99
- (1984) *Eur J Biochem* 138:9–37
- Faller P (2009) *ChemBioChem* 10:2837–2845
- Hureau C, Faller P (2009) *Biochimie* 91:1212–1217
- Kozłowski H, Luczkowski M, Remelli M, Valensin D (2012) *Coord Chem Rev* 256:2129–2141



21. Cherny RA, Atwood CS, Xilinas ME, Gray DN, Jones WD, McLean CA, Barnham KJ, Volitakis I, Fraser FW, Kim YS, Huang XD, Goldstein LE, Moir RD, Lim JT, Beyreuther K, Zheng H, Tanzi RE, Masters CL, Bush AI (2001) *Neuron* 30:665–676
22. Bar-Or D, Rael LT, Lau EP, Rao NK, Thomas GW, Winkler JV, Yuki RL, Kingston RG, Curtis CG (2001) *Biochem Biophys Res Commun* 284:856–862
23. Gum ET, Swanson RA, Alano C, Liu J, Hong S, Weinstein PR, Panter SS (2004) *Stroke* 35:590–595
24. Agostinho P, Cunha RA, Oliveira C (2010) *Curr Pharm Des* 16:2766–2778
25. Hu X, Zhang Q, Wang W, Yuan Z, Zhu X, Chen B, Chen X (2016) *ACS Chem Neurosci* 7:1255–1263
26. Miura T, Satoh T, Hori-i A, Takeuchi H (1998) *J Raman Spectrosc* 29:41–47
27. Miura T, Suzuki K, Kohata N, Takeuchi H (2000) *Biochemistry* 39:7024–7031
28. Takeuchi H (2003) *Biopolymers* 72:305–317
29. El Khoury Y, Dorlet P, Faller P, Hellwig P (2011) *J Phys Chem B* 115:14812–14821
30. Andrushchenko VV, Vogel HJ, Prenner EJ (2007) *J Pep Sci* 13:37–43
31. Barth A, Zscherp C (2002) *Q Rev Biophys* 35:369–430
32. Barth A (2000) *Prog Biophys Mol Biol* 74:141–173
33. Hasegawa K, Ono T-A, Noguchi T (2000) *J Phys Chem B* 104:4253–4265
34. Hasegawa K, Ono T, Noguchi T (2002) *J Phys Chem A* 106:3377–3390
35. Torreggiani A, Bonora S, Fini G (2000) *Biopolymers* 57:352–364
36. Takeuchi H (2011) *Anal Sci* 27:1077–1086
37. Sóvágó I, Várnagy K, Lihí N, Grenács Á (2016) *Coord Chem Rev* 327–328:43–54
38. Farkas E, Sovago I, Gergely A (1983) *Dalton Trans* 1983:1545–1551